PHYSICAL REVIEW A 94, 013609 (2016)

Onset of transverse instabilities of conÞned dark solitons

M. A. Hoefer[1,*] and B. Ilan[2,•]
[1]Department of Applied Mathematics, University of Colorado, Boulder, Colorado 80309, USA
[2]School of Natural Sciences, University of California - Merced, Merced, California 95343, USA
(Received 3 May 2016; published 15 July 2016)

We investigate propagating dark soliton solutions of the two-dimensional defocusing nonlinear Schrödinger or Gross-Pitaevskii (NLS-GP) equation that are transversely con ned to propagate in an in nitely long channel. Families of single, vortex, and multilobed solitons are computed using a spectrally accurate numerical scheme. The

where $E(m$

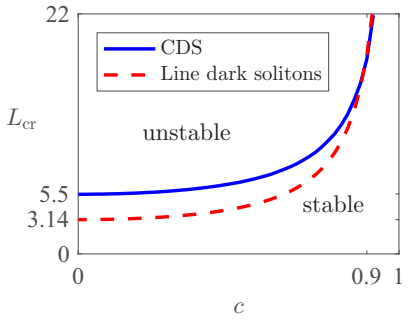

FIG. 9. Critical con nement widths as functions of propagation speed $L_{\rm cr}(c$

increases beyond a critical threshold. In general, the multilobed CDSs are all unstable.

Finally, to test the linear stability theory, we carry out direct numerical simulations of the NLS-GP equation (1) with impenetrable walls and initial conditions that correspond to a CDS with a small amount of "noise." The numerical method is explained in Appendix C. Figure 10 presents some of the results, which show that $L_{cr}(c)$, obtained from spectral analysis, is indeed the critical con nement width for nonlinear stability. Moreover, these simulations reveal that, when $L_y > L_{cr}$, the CDS undergoes a snaking instability and can break up into a single solitonic vortex as in Fig. 10(b) or counterpropagating solitonic vortex pairs as in Fig. 10(c).

VI. CONCLUSIONS

The critical con nement widths for stabilizing propagating dark solitons in the defocusing or repulsive NLS-GP equation were obtained using spectral analysis and veri ed by direct computations. The results show that (i) for a given con nement width, the faster the solitons propagate, the more stable they become; (ii) impenetrable walls are more stabilizing than zero ux boundaries. These results generalize upon previous studies for black (nonpropagating) dark solitons and gray (propagating) dark solitons. As part of this analysis, we also analytically obtained approximate con ned dark solitons with impenetrable walls. This approximation was used to show that con ned dark solitons have a reduced speed compared with the uncon ned case, which is consistent with and may help to explain experimental observations in BECs.

APPENDIX A: COMPUTING THE CDS

We compute CDS bound-state solutions of (2a) and (2b) using a spectrally accurate quasi-Newton approach [36]. It is convenient to break up (7) into its real and imaginary parts by taking $u_{cds} = u + iv$ where u, v are real valued,

$$\begin{aligned} F(u,v) &= \tfrac{1}{2}u_{xx} + cv_x - (u^2+v^2-\mu)u = 0, \\ G(u,v) &= \tfrac{1}{2}v_{xx} - cu_x - (u^2+v^2-\mu)v = 0. \end{aligned} \tag{A1}$$

We seek solutions that rapidly asymptote to the uniform background state

$$u^2(x,y) + v^2(x,y) \to u_b(y)^2, \quad |x| \to \infty. \tag{A2}$$

The far- eld density normalization (10) determines the chemical potential μ to be its background value (A4).

We solve Eq. (A1) using discrete cosine and sine transforms achieving rapid (spectral) convergence. For completeness, we include a discussion of these transforms in the following subsection.

Discrete transforms

In order to evaluate Eq. (7) on a nite grid with spectral accuracy, we introduce the half grid points on $[-L_x/2, L_x/2] \times [-L_y/2, L_y/2]$,

$$\begin{aligned} x_i &= -\frac{L_x}{2} + \frac{2i-1}{2}\Delta x, \quad \Delta x = \frac{L_x}{N_x}, \quad i = 1,2,\ldots,N_x, \\ y_j &= -\frac{L_y}{2} + \frac{2j-1}{2}\Delta y, \quad \Delta y = \frac{L_y}{N_y}, \quad j = 1,2,\ldots,N_y. \end{aligned} \tag{A3}$$

The truncation of $\mathbb{R}$ to $(-L_x/2, L_x/2)$ is achieved by employing Neumann boundary conditions,

$$u_x(\pm L_x/2, y) = 0, \quad v_x(\pm L_x/2, y) = 0, \tag{A4}$$

which are natural for dark solitons that rapidly decay to differing constant values for $x \to \pm\infty$. To evaluate derivatives and simultaneously satisfy the boundary conditions, we approximate the solution with a truncated cosine series expansion in x and a truncated sine series expansion in y,

$$\begin{aligned} u(x,y) &\approx \frac{2}{\sqrt{(N_x-1)(N_y-1)}} \\ &\times \sum_{n=1}^{N_x}\sum_{m=1}^{N_y} \hat{u}_{n,m} \cos\frac{(x+L_x/2)(n-1)}{L_x} \\ &\times \sin\frac{(y+L_y/2)(m-1)}{L_y}, \end{aligned} \tag{A5}$$

$$\begin{aligned} v(x,y) &\approx \frac{2}{\sqrt{(N_x-1)(N_y-1)}} \\ &\times \sum_{n=1}^{N_x}\sum_{m=1}^{N_y} \hat{v}_{n,m} \cos\frac{(x+L_x/2)(n-1)}{L_x} \\ &\times \sin\frac{(y+L_y/2)(m-1)}{L_y} \end{aligned}$$

where $a > 0$ is an acceleration parameter. The preconditioner is applied efficiently using the DCST,

$$L^{-1}F = \begin{bmatrix} S_{k_y}^{-1} C_k^{-1} \left\{ \frac{a\tilde{-}\mu + \frac{1}{2}(k^2 + k_y^2)}{(a\tilde{-}\mu + \frac{1}{2}(k^2 + k_y^2))^2 \tilde{-} c^2 k^2} S_y C\{F\} \right\} + S_{k_y}^{-1} S_k^{-1} \left\{ \frac{\tilde{-} ck}{(a\tilde{-}\mu + \frac{1}{2}(k^2 + k_y^2))^2 \tilde{-} c^2 k^2} S_y C\{G\} \right\} \\ S_{k_y}^{-1} C_k^{-1} \left\{ \frac{a\tilde{-}\mu + \frac{1}{2}(k^2 + k_y^2)}{(a\tilde{-}\mu + \frac{1}{2}(k^2 + k_y^2))^2 \tilde{-} c^2 k^2} S_y C\{G\} \right\} \tilde{-} S_{k_y}^{-1} S_k^{-1} \left\{ \frac{\tilde{-} ck}{(a\tilde{-}\mu + \frac{1}{2}(k^2 + k_y^2))^2 \tilde{-} c^2 k^2} S_y C\{F\} \right\} \end{bmatrix}. \quad \text{(A11)}$$

The stopping (convergence) criteria for Newton's method is an l^2 norm of the residual less than 10^{-13}. An example convergence plot is presented in Fig. 10. The reference "exact" solution is computed on a large ($L_x = 60$), very fine grid ($\Delta = 0.1$). The black soliton ($c = 0$) exhibits the strongest localization and requires $L_x \geq 40$ to achieve the highest accuracy. The gray soliton with $c = 0.5$ is broader than the dark soliton and hence requires a slightly longer channel width $L_x \geq 50$ to achieve the highest accuracy. For both the black and gray solitons a grid spacing of $\Delta x = \Delta y = 0.15$ achieves an a